Poroelastic Behavior of Trabecular Bone: The Effect of Strain Rate

Jung Hwa Hong* and Sam Hong Song**

(*Received July 5, 1997*)

A one dimensional poroelastic model of trabecular bone was developed to investigate the pore pressure effect on mechanical behavior. The poroelastic properties were determined based upon the assumed drained Poisson's ratio of 0.3 and the experimental results reported in the literature. Even though the free escape of the fluid through the loading end was allowed during deformation, model predictions showed that the pore pressure generation within the trabecular bone would cause significant variations in total stress. The total stress increase resulted in a stiffening of the trabecular bone, which supports the concept of hydraulic stiffening that has been advocated by several investigators. Model predictions showed a good agreement to the mechanical behaviors of trabecular bone specimens with marrow in a uniaxial strain condition observed in a previous study. These results support the hypothesis that the trabecular bone is poroelastic and the pore pressure effect on the mechanical behavior at the continuum level is significant. Thus, the incorporation of the fluid effect in future studies is recommended to improve our understanding of trabecular bone mechanics.

Key Words: Biomechanics, Trabecular Bone Mechanics, Theory of Poroelasticity, Uniaxial Strain Condition, Strain Rate Effect, Stiffening Phenomena

1. Introduction

Bone is the primary structural element of the human body. It provides support for external and internal loading. Bone is a composite material composed of porous solid and fluid phases. Macroscopically, bone is characterized into two distinct structures: trabecular bone and cortical bone. Trabecular bone has a highly viscous fluid (67 times of water viscosity at 37°C), while cortical bone is saturated with a less viscous fluid (approximately equal to water viscosity at 37°C) (Bryant, 1988). The pore space of bone is known to be continuous to allow interstitial fluid flow in bone (Hughes et al., 1978). The porosity of trabecular bone is more than 0.7, while that of cortical bone shows a porosity of less than 0.2. Therefore, trabecular bone can be defined as a highly porous structure filled with a highly viscous fluid, while cortical bone can be classified as a less porous structure with a less viscous fluid.

Trabecular bone occupies the inner most parts of the bone to provide mechanical function for load bearing. However, aging and pathological conditions (osteoporosis, osteonecrosis, and osteoarthritis) can reduce stiffness and strength of the trabecular bone. As a result, the reduction of mechanical properties of the trabecular bone causes increased frequencies of fracture to the hip, spine, and wrist, which reflects tremendous sociological and economic implications (Keaveny and Hayes, 1993). To treat fracture, orthopaedic fixation implants and arthroplasties have been placed primarily in trabecular bone sites. However, loosening and mismatch between trabecular bone and the devices have resulted in significant clinical problems after expensive orthopaedic surgical procedures (Snyder, 1991). Knowledge of the mechanical behavior of trabecular bone may enhance understanding of important orthopaedic problems. As a result, experimental and theoretical biomechanical studies of trabecular bone have

* Technology Center, Samsung Motors Inc.
** Department of Mechanical Engineering, Korea University

been performed to characterize elastic behavior of trabecular bone. The investigations have contributed to prediction of mechanical behavior of trabecular bone, and suggested better understanding of effects of the aging and pathological conditions of trabecular bone on its changes of mechanical properties.

Unlike elastic materials, however, trabecular bone exhibits time-dependent mechanical behavior such as stress relaxation, creep, influence of strain and loading rate input on its mechanical properties, and phase-shift phenomena under dynamic loading input (Carter and Hayes, 1977; Ducheyne *et al.*, 1977; Linde *et al.*, 1991; Luo *et al.*, 1993; Nowinski, 1972; Ochoa *et al.*, 1991; Schoenfeld *et al.*, 1974; Tateishi, 1979). The theory of viscoelasticity has been used to explain the inelastic and time- dependent behavior of trabecular bone (Deligianni, 1994; Kafka and Jirovâ 1983). However, the theory of viscoelasticity cannot characterize a mechanical role of interstitial fluid flow and pore pressure generation due to the fluid phase occupying more than 70% of the volume of trabecular bone. As a theory comprising the fluid phase of bone, the theory of poroelasticity has been used to account for coupled interaction between the porous solid and viscous fluid. Zhang and Cowin (1994) investigated the bending behavior of a cortical bone beam under axial compression and cyclic bending loads using the theory of poroelasticity (Rice and Cleary, 1976), . They demonstrated a significant role of the fluid phase in increasing the load-bearing capacity of cortical bone under dynamic loading. The authors suggested that the load bearing role of pore pressure would be even more significant in trabecular bone. Harrigan and Hamilton (1993) also employed the theory of poroelasticity (Rice and Cleary, 1976) to investigate the role of pore pressure in generating electrical potential and shear stress of cortical bone, that may be associated with its remodeling process. When trabecular bone is subjected to an external load, however, its time-dependent behavior has not been fully investigated using the theory of poroelasticity. Particularly, the strain rate effect (or loading rate) on changes of total stress behavior and mechanical properties of trabecular bone that is most likely due to the role of the intraosseous fluid (Luo *et al.*, 1993, Ochoa *et al.*, 1991) has not been studied using poroelasticity.

The purpose of this study is to understand the pore pressure effect in trabecular bone on its strain rate-dependent mechanical behavior. In this study, a one-dimensional poroelastic model of trabecular bone was developed by solving the poroelastic constitutive and diffusion equations (Rice and Cleary, 1976) in a uniaxial strain condition. The model was used to investigate the effect of pore pressure generation on changes of total stress behavior and mechanical properties of trabecular bone with variation of the poroelastic properties. Model predictions were also validated using reported experimental data (Carter and Hayes, 1977).

2. Poroelastic Model of Trabecular Bone in a Uniaxial Strain Condition

2.1 Poroelastic theory

Stress exerted on a control volume element of a fluid-filled porous material (total stress) produces both strains and changes in pore pressure in the control element. Rice and Cleary (1976) reformulated the relationship among the total stress, strain, and pore pressure using unique material parameters (Table 1). Assuming the isotropy of the poroelastic material, the constitutive equations were defined as:

$$\sigma_{ij}+\frac{3p(\nu_u-\nu)}{B(1-2\nu)(1+\nu_u)}\delta_{ij}=2G\varepsilon_{ij}+\frac{2G\nu}{1-2\nu}\varepsilon_{kk}\delta_{ij} \quad (1)$$

where σ_{ij}=total stress tensor (MPa); ε_{ij}=strain

Table 1 Model parameters in the governing equations used for the modeling of poroelastic material.

Parameters	
G	Drained shear modulus (MPa)
ν	Drained Poisson's ratio
ν_u	Undrained Poisson's ratio
B	Skempton's pore pressure coefficient
$\varkappa$	Permeability Coefficient (m^2/MPa/sec)

tensor; p=pore pressure (MPa); δ_{ij}=Kronecker delta (if $i=j$, then $\delta_{ij}=1$, if $i\neq j$ then $\delta_{ij}=0$); and i, $j=1$, 2, 3 (the summation convention applies when repeated indices are used).

The diffusion equation that governs pore pressure generation with volumetric deformation of the control element is (Detournay and Cheng,, 1993):

$$\frac{\partial p}{\partial t}-\frac{2\chi GB^2(1-2\nu)(1+\nu_u)^2}{9(\nu_u-\nu)(1-2\nu_u)}\nabla^2 p = -\frac{2GB(1+\nu_u)}{3(1-2\nu_u)}\frac{\partial \varepsilon_{kk}}{\partial t} \quad (2)$$

where t=time; $\nabla^2=\sum_{i=1}^{3}\frac{\partial^2}{\partial x_i^2}$(the Laplacian operator); and ε_{kk}=the trace of the strain tensor or volumetric strain.

When a poroelastic material deforms without generating pore pressure (p=0.0), Eq. (1) becomes the constitutive equation for an isotropic elastic solid material:

$$\sigma_{ij}=2G\varepsilon_{ij}+\frac{2G\nu}{1-2\nu}\varepsilon_{kk}\delta_{ij} \quad (3)$$

where G=shear modulus and ν=Poisson's ratio. Such a deformation with zero pore pressure generation can occur when a quasi-static load is applied to poroelastic material in a drained condition in which the interstitial fluid can flow across the boundary with no resistance. Thus, this was called a drained deformation, and G and n were named the shear modulus and the drained Poisson's ratio, respectively.

The other asymptotic behavior of poroelastic material is called undrained deformation, since it occurs in an undrained condition in which the interstitial fluid is totally prevented from flowing out of the control volume element across the boundary. During undrained deformation, a poroelastic material can be treated as an elastic material with the same shear modulus (G) but different Poisson's ratio, i. e., the undrained Poisson's ratio (ν_u). The corresponding constitutive equations can be expressed as (Detournay and Cheng,, 1993):

$$\sigma_{ij}=2G\varepsilon_{ij}+\frac{2G\nu_u}{1-2\nu_u}\varepsilon_{kk}\delta_{ij} \quad (4)$$

The theoretical range of ν_u is $\nu\leq\nu_u\leq 0.5$.

Skempton's coefficient (B) was defined as the ratio of the pore pressure increment (Δp) to the mean stress increment ($\Delta\delta_{kk}/3$) during an undrained deformation (Green and Wang, 1986): $B=-3\Delta p/\Delta\delta_{kk}$. Thus, B indicates the load bearing capability of the fluid constituent that is caused by the restricted fluid flow across the boundary. In general, B varies from 0.0 to 1.0 (Detournay and Cheng,, 1993).

The relationship between B and ν_u is $\alpha B=[3(\nu_u-\nu)]/[(1-2\nu)(1+\nu_u)]$, where α is the Biot coefficient of effective stress and ν is the drained Poisson's ratio. B and ν_u are known to be related with the compressibility of both solid and fluid constituents. Their values represent the poroelastic effects such as the sensitivity of the volumetric response to the rate of loading and the rate of pore pressure generation. For example, B and ν_u values are 1.0 and 0.5, respectively, for a poroelastic material consisting of the incompressible solid and fluid constituents in which the poroelastic effects are strongest. When the fluid constituent becomes more compressible, some of the poroelastic effects disappear, and B and ν_u become closer to 0.0 and ν, respectively.

The permeability coefficient (χ) is a well known parameter which describes how the interstitial fluid can flow through the pores in a poroelastic material. χ is known to be sensitive to the viscosity of the fluid, as well as to the geometrical factors such as pore size and tortuosity (Scheidegger, 1957). However, the permeability coefficient is an intrinsic property that needs to be measured separately from the elastic property measurements.

2.2 Poroelastic governing equations of trabecular bone

The following assumptions needed to be made for the poroelastic modeling of trabecular bone: 1) Trabecular bone is an isotropic elastic solid matrix saturated with a Newtonian fluid; and 2) Pores are uniformly distributed throughout the volume. With these assumptions and appropriate poroelastic property values, the poroelastic governing Eqs. (1) and (2) were solved for various loading conditions to obtain a uniaxial strain

poroelastic model of trabecular bone.

A uniaxial strain condition and uniform deformation throughout the control element were assumed to obtain an analytic solution. The cylindrical trabecular specimen boundary was assumed to be confined except for the single axial end where the load was applied. When a constant strain rate ($\dot{\varepsilon}_3$) was used for axial compressive loading, axial strain ($\varepsilon_3=\dot{\varepsilon}_3 t$) and lateral strains ($\varepsilon_1$ and ε_2) vanished. Then, the stress- strain relationship (Eq. 1) became:

$$\sigma_3=\frac{2G(1-\nu)}{1-\nu}\dot{\varepsilon}_3 t-\frac{3(\nu_u-\nu)}{B(1-2\nu)(1+\nu_u)}p \quad (5)$$

and

$$\sigma_1=\sigma_2=\frac{2G\nu}{1-2\nu}\dot{\varepsilon}_3 t-\frac{2(\nu_u-\nu)}{B(1-\nu)(1+\nu_u)}p. \quad (6)$$

The diffusion equation (Eq. 2) became:

$$\frac{\partial p}{\partial t}-\frac{2\kappa GB^2(1-2\nu)(1+\nu_u)^2}{9(\nu-\nu)(1-2\nu_u)}\frac{\partial^2 p}{\partial x_3^2}=-\frac{2GB(1+\nu_u)}{3(1-2\nu_u)}\frac{\partial \varepsilon_3}{\partial t}. \quad (7)$$

Initial and boundary conditions required to solve the diffusion equation for the pore pressure (p) were: 1) no initial pore pressure ($p(x_3, 0)=0$); 2), $p(0, t)=0$, i. e., pore pressure is always zero at the loading end ($x_3=0$); and 3) $\partial p(L, t)/\partial x_3=0$, i. e., no pressure gradient, suggesting that no fluid flow is allowed across the distal end (at $x_3=L$), where L is the length of the fluid-saturated porous material.

The diffusion Eq. (7) was solved under these boundary and initial conditions to predict pore pressure generation resulting from constant strain rate loading ($\dot{\varepsilon}_3$) using the method of separation of variables. The solution for the pore pressure was

$$p(x_3, t)=-\sum_{n=1}^{\infty}\frac{6(\nu_u-\nu)\dot{\varepsilon}_3}{\kappa BL\omega_n^3(1-2\nu)(1+\nu_u)}(1-e^{-\Psi\omega_n^2 t})\sin(\omega_n x_3) \quad (8)$$

where eigenvalues $\omega_n=(2n-1)\pi/2L$ and constant $\Psi=\frac{2\kappa GB^2(1-2\nu_u)(1+\nu_u)^2}{9(1-2\nu)(\nu_u-\nu)}$. Substitution of Eq. (8) into Eq. (5) allowed an expression of the total stress in response to an applied strain in a uniaxial strain condition:

$$\sigma_3=\frac{2G(1-\nu)}{1-2\nu}\dot{\varepsilon}_3 t-\sum_{n=1}^{\infty}\frac{18(\nu_u-\nu)^2\dot{\varepsilon}_3}{\kappa B^2L\omega_n^3(1-2\nu)^2(1+\nu_u)^2}(1-e^{-\Psi\omega_n^2 t})\sin(\omega_n x_3) \quad (9)$$

Whenever required for analysis purposes, the first five terms in the infinite summation in Eq. (8) or (9) were used to obtain the pore pressure or total stress values.

2.3 Estimation of poroelastic parameters

Little experimental data for poroelastic properties of trabecular bone are available at present. It is possible, however, to estimate various properties on the basis of reported experimental results (Carter and Hayes, 1977; Ochoa and Hillberry, 1992) with an assumed drained Poisson's ratio (ν) of 0.3. This assumption has been used by others (Goel *et al.*, 1978) in modeling trabecular bone, although wide variations of Poisson's ratio also have been reported in the literature.

Carter and Hayes (1977) conducted confined compression tests (Fig. 1) of human trabecular bone specimens with and without marrow at uniaxial strain rates ranging from 0.001 to 10 per second. The compressive modulus of specimens with marrow was similar to that of specimens without marrow (56.6 MPa vs. 54 MPa) at a strain rate of 0.001/sec. The loading with the slowest strain rate seemed to result in a drained deformation in which the marrow escaped freely through the porous loading platen without gener-

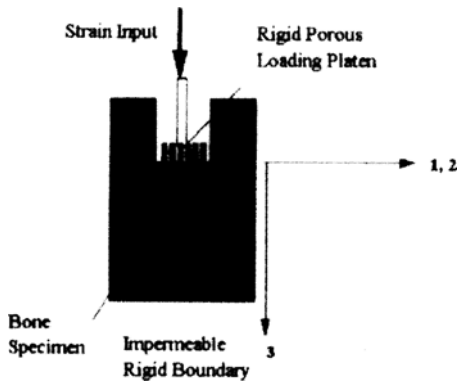

Fig. 1 The experimental setup in a uniaxial strain condition (Carter and Hayes, 1977)

ating pore pressure. This suggested that the compressive modulus at the slowest strain rate represented the mechanical behavior of the solid constituent. From equation (3) and the reported compressive modulus of 56.6 MPa, $2G(1-\nu)/(1-2\nu)=56.6$. Then, assuming $\nu=0.3$, the estimated value of the shear modulus G was 16.17 MPa.

At the highest strain rate of 10/second, the compressive modulus of the specimens with marrow in situ showed a 400% increase compared to those without marrow (211 MPa vs. 54 MPa) (Carter and Hayes, 1977). This compressive modulus increase seemed to result primarily from the restricted flow of marrow through the pores in the platen with a fast loading rate. Thus it was reasonable to assume that an undrained deformation occurred in the specimen tested at a strain rate of 10 per second. From Eq. (4) and an estimated value of $G=16.17$ MPa, the undrained Poisson's ratio, ν_u, was determined to be 0.459.

The exact value of Skempton's coefficient (B) could not be determined due to the lack of experimental information. However, its range of 0.817 to 1.0 could be predicted using the theoretical range of B and the Biot coefficient of effective stress (α) (from 0 to 1) and the relationship (Detournay and Cheng, 1993): $\alpha B=[3(\nu_u-\nu)]/[(1-2\nu)(1-\nu_u)]$. Skempton's coefficient was assumed to be 0.91 (midpoint of the theoretically possible range) whenever required for model predictions.

The permeability coefficient (χ) of bovine proximal tibial trabecular bone was measured by Ochoa and Hilberry (1992). The mean value of χ ($\pm$SD) was 3.54 ($\pm$1.76) $\times 10^{-5}$m^2/MPa/sec. This mean value was used for our analysis which required values for k since it would be closer to the permeability of human trabecular bone than the known values of other materials such as cortical bone, cartilage, and rocks. A permeability range from 1.0×10^{-7} to 1.0×10^{-3}m^2/MPa/sec was used to additionally investigate the effect of permeability on the poroelastic characteristics of trabecular bone. The lower limit was determined from the assumption that trabecular bone has a larger permeability than bovine and canine cortical bone (Johnson *et al*, 1982; Li *et al.*, 1987). The upper limit was assumed to be 100 times larger than the measured permeability of bovine trabecular bone (Johnson *et al*, 1982).

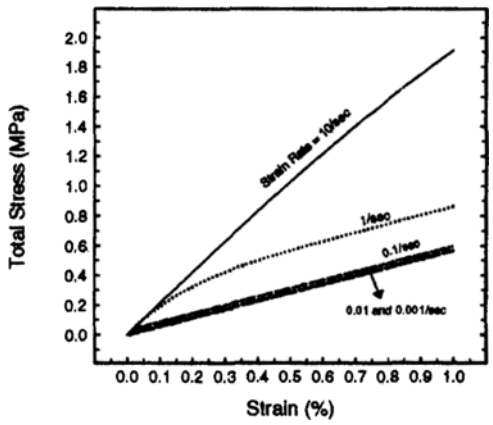

Fig. 2 Total stress-strain curves predicted from the poroelastic model at various strain rates when $G=16.17$ MPa; $\nu=0.3$; $\nu_u=0.459$; $B=0.91$; and $\chi=3.54\times10^{-5}$m^2/MPa/sec. Time durations to reach the strain of 1% were 10, 1, 0.1, 0.01, and 0.001 second when strain rate inputs were 0.001, 0.01, 0.1, 1, and 10 per second, respectively.

3. Results and Discussion

3.1 Poroelastic behavior of trabecular bone

The poroelastic behavior of trabecular bone was investigated using Eq. (9). Poroelastic property values were estimated in terms of total stress changes resulting from the strain inputs. Figure 2 illustrates the total stress-strain curves predicted from the poroelastic model at various strain rates. Almost linear relationship was expected at slower strain rates of 0.001 and 0.01/sec due to the negligible effect of pore pressure (drained deformation). At the fastest strain rate, the total stress -strain relationship was also almost linear, which represented the undrained deformation. The nonlinear deformation at the intermediate strain rate 1.0/sec was predicted to result in the nonlinear total stress-strain relationship due to the pore pressure generation.

In uniaxial strain conditions, the total stress

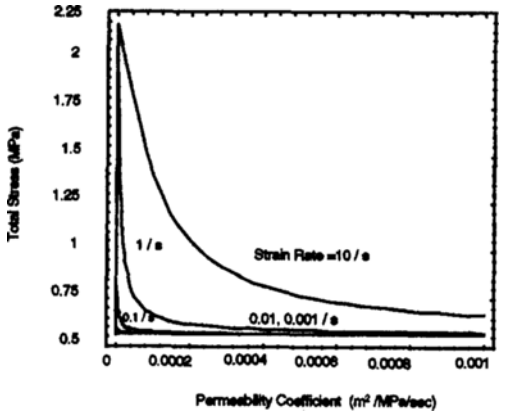

Fig. 3 Variation of total stress vs. (a) permeability when B=0. 91; and (b) Skempton's coefficient when $k=3.54\times10^{-5}m^2/MPa/sec$. The total stress values in response to a 1% strain deformation were used to obtain these plots.

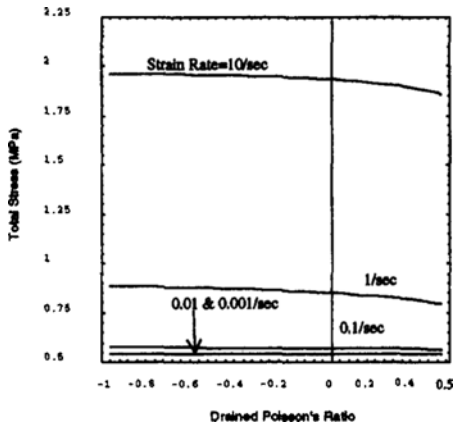

Fig. 4 Variation of total stress (MPa) vs. drained Poisson's ratio when B=0.91 and $\chi=3.54\times10^{-5}m^2/MPa/sec$.

-strain behaviors were significantly affected by the applied strain rate as shown in Fig. 2 even though the fluid was assumed to escape from the control element with no restriction. These total stress variations resulted from pore pressure changes generated during deformation. The increased total stress values in response to the same strain deformation at the faster strain rate compared to those at the slow strain rate supports the concept of hydraulic strengthening that has been advocated by several investigators (Carter and Hayes, 1977; Downey *et al.*, 1988; Ducheyne *et al.*, 1977; Ochoa *et al.*, 1991).

3.2 The effects of poroelastic parameters on total stress behavior

The effect of permeability on total stress was also investigated in this study since the amount of pore pressure generated by fluid constituent can vary as a function of the permeability coefficient. Total stress decreased with increasing permeability coefficient at all strain rate inputs (Fig. 3), and much greater effect was predicted in the permeability coefficient range of less than 2.0×10^{-4} $m^2/MPa/sec$. Since the permeability coefficient of trabecular bone would be in this range of smaller values, the permeability changes in trabecular bone may affect pore pressure generation substantially.

Equations (8) and (9) also demonstrated that pore pressure generation and total stress can vary as functions of the undrained Poisson's ratio and Skempton's coefficient that are associated with the compressibility of both solid and fluid constituents. However, these two parameters are correlated with each other, and it was impossible to perform a parametric study to investigate the effect of these parameter value changes on the pore pressure generation.

The effect of varying drained Poisson's ratio (ν) on total stress was also investigated because a large variation in measured values of ν has been reported in the literature although ν has been assumed to be 0.3 in a previous study (Goel *et al.*, 1978). For this analysis, the values of G, ν_u, and B were changed corresponding to the various values of ν to maintain the same elastic modulus reported in Carter and Hayes' study (1977), while the permeability coefficient value was fixed at 3.54×10^{-5} ($m^2/MPa/sec$). Figure 4 illustrates total stress behavior at various strain rates when ν varies within the theoretically possible range from -1.0 to 0.5 for a linear elastic and isotropic material. As shown in Fig. 4, total stress decreased with increasing ν values, while the effect of varying ν on total stress became greater at higher strain rates. However, variations in ν values did not result in dramatic total stress behavior even at the highest strain rate

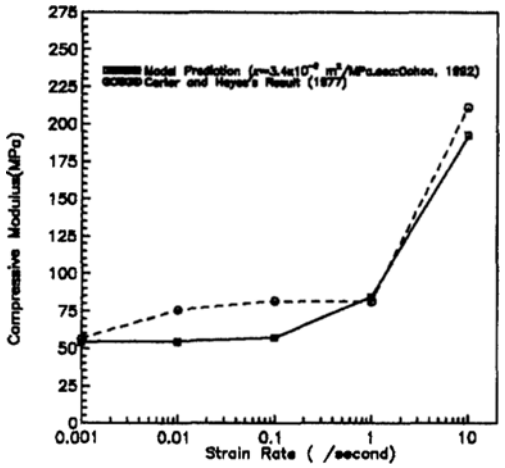

Fig. 5 Variation of predicted compressive modulus vs. strain rate.

3.3 Hydraulic Stiffening Effect

The enhancement of the compressive modulus (or stiffness) at faster strain rates has been observed by Carter and Hayes (1977). Similar variations in compressive modulus were predicted from the poroelastic model as shown in Figure 5 when the previously estimated model parameter values were used for model predictions. An exception was the increase in compressive modulus from the strain rate of 0.01 per second. The increases at strain rates of 0.01 and 0.1/sec seemed to occur primarily due to the use of different boundary conditions. Free fluid flow across the loading boundary was allowed in the model prediction, whereas the flow of marrow through the loading platen was restricted in the experiment since the size of platen pores were much smaller than those of the trabecular bone (Carter and Hayes, 1977). Similar stiffening effects of faster loading also have been observed even in unconfined uniaxial stress tests conducted in other studies (Carter and Hayes, 1977; Linde *et al.*, 1991).

4. Conclusion

In this study, the theory of poroelasticity was used to investigate the strain rate effect on the total stress behavior and changes of stiffness of trabecular bone caused by the pore pressure generation. A one-dimensional poroelastic model in a uniaxial strain condition was developed to simulate the compressive tests of trabecular bone with and without marrow. The strain rate-dependent mechanical behavior of trabecular bone was described by either the total stress or the compressive modulus variations in response to the applied strain. The conclusions from the present investigation can be summarized as follows:

(1) The total stress-strain behavior of trabecular bone was greatly affected by the applied strain rate. The predicted total stress increased significantly as strain rate input increased. The increased total stress resulted from the pore pressure effect as predicted by Eq. (9).

(2) The compressive modulus of trabecular bone linearly increased as applied strain rate increased. This stiffening behavior of trabecular bone showed good agreement to the mechanical behavior of trabecular bone specimens with marrow in a uniaxial strain condition observed in a previous experimental study.

(3) This study showed that the strain rate dependent stiffening of trabecular bone can be accurately simulated to understand the effect of pore pressure generation on the total stress and stiffening behavior using the theory of poroelasticity. Future experimental study is required to measure the five poroelastic properties for developing a more detailed poroelastic model of trabecular bone.

References

Bryant, J. D., 1988, "On the Mechanical Function of Marrow in Long Bone," *Eng. Med.*, Vol. 17, pp. 55~58.

Carter, D. R. and Hayes, W. C., 1977, "The Compressive Behavior of Bone as a Two-phase Porous Structure," *J. Bone Joint Surg.*, Vol. 59A, pp. 954~962.

Deligianni, D. D., Maris, A. and Missirlis, Y. F., 1994, "Stress Relaxation Behavior of Trabecular Bone Specimens," *J. Biomech.*, Vol. 27, pp. 1469~1476.

Detournay, E. and Cheng, H. D., 1993, *Fundamentals of poroelasticity. Comprehensive Rock*

Engineering: Principles, Practice and Projects (Hudson, J. edited), Vol. 2, pp. 113~171, Pergamon Press, New York.

Downey, D. J., Simkin, P. A. and Taggart, R., 1988, "Compressive Loading Raises Intraosseous Pressure in the Femoral Head," *J. Bone Joint Surg.*, Vol. 70A, pp. 871~877.

Ducheyne, P., Heymans, L., Martens, M., Aernoudt, E. de Meester, P. and Mulier, J. C., 1977, "The Mechanical Behavior of Intracondylar Cancellous Bone of the Femur at Different Loading Rates," *J. Biomech., Vol.* 10, pp. 747~762.

Goel, V. K., Valliappan, S. and Svensson, N. L., 1978, "Stresses in the Normal Pelvis," *Comput. Biol. Med.*, Vol. 8, pp. 91~104.

Green, D. H. and Wang, H. F., 1986, "Fluid Pressure Response to Undrained Compression in Saturated Sedimentary Rock," *Geophys.*, Vol. 51, pp. 948~956.

Harrigan, T. P. and Hamilton, J. J., 1993, "Bone Strain Sensation Via Transmembrane Potential Changes in Surface Osteoblasts: Loading Rate and Microstructural Implications," *J. Biomech.*, Vol. 26, pp. 183~200.

Hughes, M. S., Davies, R., Khan, R. and Kelly, P., 1978, "Fluid Space in Bone," *Clinical Orthop. Res.*, Vol. 134, pp. 332~341.

Johnson, M. W., Chakkalakal, D. A., Harper, R. A., Karz, J. L. and Rouhana, S. W. , 1982, "Fluid Flow in Bone," *J. Biomech.*, Vol. 11, pp. 881~885.

Kafka, V. and Jirová J., 1983, "A Structural Mathematical Model for the Viscoelastic Anisotropic Behavior of Trabecular Bone," *Biorheology*, Vol. 20, pp. 795~806.

Keaveny, T. M. and Hayes, W. C., 1993, "A 20-year Perspective on the Mechanical Properties of Trabecular Bone," *J. Biomech. Eng.*, Vol. 115, pp. 534~542.

Li, G., Bromk, J. T. and Kelly, P. J., 1987, "Permeability of Cortical Bone of Canine Tibiae," *Microvascular Res.*, Vol. 34, pp. 302~310.

Linde, F., Nfrgaard, P., Hvid, I., Odgaard, A. and Sfballe, K., 1991, "Mechanical Properties of Trabecular Bone. Dependence on Strain Rate," *J. Biomech.*, Vol. 24, pp. 803~809.

Luo, Z. P., Ochoa, J. A. and Hillberry, B. M., 1993, "Effect of Specimen Size on Hydraulic Stiffening of Cancellous Bone," *Tans. Orthopaedic Research Society*, Vol. 18, pp. 174.

Nowinski, J. L., 1972, "Stress Concentration Around a Cylindrical Cavity in a Bone Treated as a Poroelastic Body," *Acta Mechanica*, Vol. 13, pp. 281~192.

Ochoa, J. A., Sanders, A. P., Heck, D. A. and Hillberry B. M., 1991, "Stiffening of the Femoral Head Due to Intertrabecular Fluid and Intraosseous Pressure," *J. Biomech. Eng.*, Vol. 113, pp. 259~262.

Ochoa, J. A. and Hillberry B. M., 1992, "Permeability of Bovine Cancellous Bone," *Trans. Orthopaedic Research Society*, Vol. 17, pp. 162.

Rice, J. R. and Cleary, M. P., 1976, "Some Basic Stress-Diffusion Solutions for Fluid Saturated Elastic Porous Media with Compressible Constituents," *Res. Geophys. Space Phys.*, Vol. 14, pp. 227~241.

Scheidegger, A. E., 1957, *The Physics of Flow Through Porous Media*, University of Toronto Press, Toronto.

Snyder B. D., 1991, *Anisotropic Structure-Property Relations for Trabecular Bone*, Ph. D. Dissertation, Univ. Pennsylvania.

Tateishi, T., 1979, *Rheological characteristics of human joints. Recent research on echanical behavior solids*, pp. 179~204, Univ. Tokyo Press, Tokyo, Japan.

Zhang, D. and Cowin, S. C., 1994, "Oscillatory Bending of a Poroelastic Beam," *J. Mech. Phys. Solids*, Vol. 42, pp. 1575~1599.